

Optimized geometries for optical lattices

A,¹ B,¹ and C¹

¹Department of Physics, Harvard University, Cambridge, Massachusetts 02138, USA

This is the abstract.

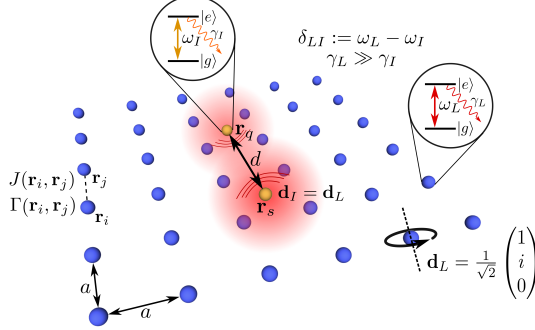


Figure 1. •

I. INTRODUCTION

II. MODEL

[arb. geometry, Green's Tensor, Couplings, Polarizations → Distance dependence, Hamiltonian, Self-energy, Ref. to Taylor's work]

We consider two-dimensional sub-wavelength lattices of quantum emitters which interact via resonant dipole-dipole interactions. The emitters are assumed to be two-level systems with a ground state $|g\rangle$ and an excited state $|e\rangle$ with a transition frequency $\omega_L = ck_L$, such that $k_L = 2\pi/\lambda_L$ denotes the related wavenumber with the resonance wavelength λ_L . Pairwise resonant dipole-dipole interactions among emitters result in collective couplings J_{ij} and collective decay rates Γ_{ij} between emitters i and j at positions \mathbf{r}_i and \mathbf{r}_j respectively, given by

$$J_{ij} = -\frac{3\pi\sqrt{\gamma_i\gamma_j}}{\omega_L} \hat{d}_i^\dagger \cdot \mathbf{Re}[\mathbf{G}(\mathbf{r}_{ij}, \omega_L)] \cdot \hat{d}_j \quad (1a)$$

$$\Gamma_{ij} = \frac{6\pi\sqrt{\gamma_i\gamma_j}}{\omega_L} \hat{d}_i^\dagger \cdot \mathbf{Im}[\mathbf{G}(\mathbf{r}_{ij}, \omega_L)] \cdot \hat{d}_j \quad (1b)$$

where γ_i and γ_j are the decay rates of the individual dipoles i and j , and $\mathbf{r}_{ij} = \mathbf{r}_i - \mathbf{r}_j$ is the displacement vector. $\mathbf{G}(\mathbf{r}_{ij}, \omega_L)$ is the Green's tensor, defined as

$$G_{\alpha\beta}(\mathbf{r}, \omega) = \frac{e^{i\omega r}}{4\pi r} \left[\left(1 + \frac{i}{\omega r} - \frac{1}{\omega^2 r^2} \right) \delta_{\alpha\beta} - \left(1 + \frac{3i}{\omega r} - \frac{3}{\omega^2 r^2} \right) \frac{r_\alpha r_\beta}{r^2} \right] - \frac{\delta(\mathbf{r})}{3\omega^2} \delta_{\alpha\beta} \quad (2)$$

d_i and d_j are the dipole polarizations, which are set to be uniformly circular, so that $\hat{d}_L = \hat{d}_I = \frac{1}{\sqrt{2}} (1 \ i \ 0)^T$

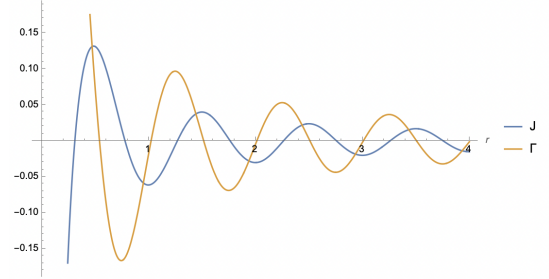


Figure 2. •

where \hat{d}_L is the polarization of the lattice dipoles, and \hat{d}_I is the polarization of any impurities. This circular polarization ensures that the dynamics of the system depend purely on the relative distances r_{ij} between pairs of dipoles, independent of their relative orientations. As a result, J_{ij} and Γ_{ij} can be written as

$$J_{ij} = -\frac{3}{8\omega_L r_{ij}} \left(\cos(\omega_L r_{ij}) + \frac{\sin(\omega_L r_{ij})}{\omega_L r_{ij}} + \frac{\cos(\omega_L r_{ij})}{(\omega_L r_{ij})^2} \right) \quad (3a)$$

$$\Gamma_{ij} = \frac{3}{4\omega_L r_{ij}} \left(\sin(\omega_L r_{ij}) - \frac{\cos(\omega_L r_{ij})}{\omega_L r_{ij}} + \frac{\sin(\omega_L r_{ij})}{(\omega_L r_{ij})^2} \right) \quad (3b)$$

In this way, collective couplings and collective decay rates (Fig. 2) depend purely on the relative distances r_{ij} between pairs of dipoles, independent of their relative orientations. Into this lattice, we place one or two lattice impurities with transition frequency $\omega_I \approx \omega_L$. The overall Hamiltonian is $H = H_L + H_{LI} + H_I$, where H_L is the Hamiltonian of the lattice, H_{LI} is the Hamiltonian for the interaction between the lattice and any impurities, and H_I is for the interactions involving just impurities. These Hamiltonians are defined such that

$$H_L = \sum_i^{N_L} \left(\omega_L - \frac{i}{2}\gamma_L \right) \sigma_i^\dagger \sigma_i + \sum_{i,j \neq i}^{N_L} \left(J_{ij} - \frac{i}{2}\Gamma_{ij} \right) \sigma_i^\dagger \sigma_j \quad (4a)$$

$$H_{LI} = \sum_i^{N_L} \sum_j^{N_I} \left[\left(J_{ij} - \frac{i}{2}\Gamma_{ij} \right) \sigma_i^\dagger s_j + \left(J_{ji} - \frac{i}{2}\Gamma_{ji} \right) s_j^\dagger \sigma_i \right] \quad (4b)$$

$$H_I = \sum_j^{N_I} \left(\omega_I - \frac{i}{2}\gamma_I \right) s_j^\dagger s_j + \sum_{i,j \neq i}^{N_I} \left(J_{ij} - \frac{i}{2}\Gamma_{ij} \right) s_j^\dagger s_j \quad (4c)$$

where N_L is the number of lattice atoms, σ_i is the lowering operator for lattice atom i , N_I is the number of impurities, and s_j is the lowering operator for impurity j .

III. SINGLE IMPURITY CASE

[Define lattices, define distances related to lattices, Γ_{eff} , constant area]

The generic form of the Hamiltonian for a given lattice of N atoms along with a single impurity is

$$H = \begin{pmatrix} & C_{LI} \\ H_L & \vdots \\ C_{IL} \dots C_{IL} & H_I \end{pmatrix} \quad (5)$$

where H_L represents the $N \times N$ matrix of terms for the lattice's own Hamiltonian, H_I is the lattice, and C_{IL} along with C_{LI} represent the coupling terms between the lattice atoms and the impurity.

Define the wavefunction such that $\psi = (b_1 \ : \ b_N \ : \ c)^T$, and assume that the lattice occupies a steady state, so that the Schrödinger equation is

$$i\hbar \begin{pmatrix} 0 \\ \vdots \\ 0 \\ \dot{c} \end{pmatrix} = \begin{pmatrix} & C_{LI} \\ H_L & \vdots \\ C_{IL} \dots C_{IL} & H_I \end{pmatrix} \begin{pmatrix} b_1 \\ \vdots \\ b_N \\ c \end{pmatrix} \quad (6)$$

This can be solved to get

$$\begin{pmatrix} b_1 \\ \vdots \\ b_N \end{pmatrix} = -H_L^{-1}C_{LI}c \quad (7)$$

Putting this back into the Schrödinger equation produces

$$\dot{c} = -i(H_I - C_{IL}^T H_L^{-1} C_{LI})c \quad (8)$$

Recognizing that $H_I - C_{IL}^T (H_L^{-1}) C_{LI} = \Sigma_I - i\frac{\gamma_I}{2}$, we can calculate the impurity's self-energy Σ_I to be

$$\Sigma_I = H_I - C_{IL}^T (H_L^{-1}) C_{LI} + i\frac{\gamma_I}{2} \quad (9)$$

The effective decay rate Γ_{eff} for an impurity in the lattice is related to this self-energy according to

$$\Gamma_{\text{eff}} = \gamma_I - 2 \operatorname{Im}[\Sigma_I] \quad (10)$$

Equipped with these mathematical tools, we consider the full range of non-centered Bravais lattices, for both interstitial and substitutional impurity positions, as illustrated in Fig. 3. In order to reasonably compare lattices of differing geometries, we ensure that all plaquettes possess the same area throughout all possible transformations.

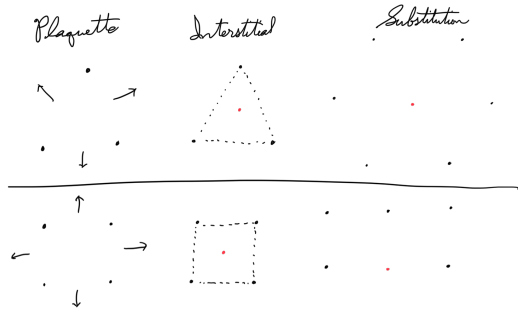


Figure 3. • [This needs to be remade so that a top line illustrates all four Bravais lattices, and a line below that illustrates the difference between the substitutional and interstitial cases. A brute force version of the bottom lines would just be to show the full lattices for each case, so that the figure later on of the substitutional triangular case could be incorporated as one amongst the eight full lattices depicted on the bottom two lines. It would at least be thorough.]

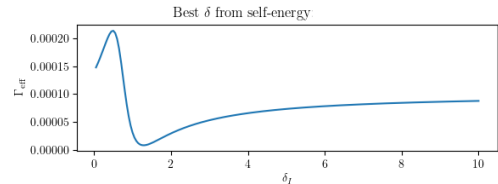


Figure 4. •

A. Interstitial

Consider a finite square lattice, with an inter-atomic spacing of $a = 0.2$ times the lattice's resonant wavelength. Compare this to the other Bravais lattices: a triangular lattice, a monoclinic lattice defined over θ from $\pi/2$ to 0, and a rectangular lattice with a scaling factor μ such that the horizontal sidelength of its rectangular plaquette is μa . [Which variable do we want for scaling? Does μ work?] To ensure that the plaquettes of all of these lattices have the same area, we set the sidelength of the triangular plaquettes to $\frac{2}{3^{1/4}}a$, the height of monoclinic plaquettes to a for all θ , and the height of the rectangular plaquettes to a/μ .

For an interstitial impurity, the position of the impurity in the plaquette along with its detuning relative the lattice's resonant frequency determine its decay properties. Detuning is defined as $\delta_{LI} = \omega_I - \omega_L$. For a given impurity position, δ_{LI} can be chosen to give optimal Γ_{eff} , by minimizing along a curve such as Fig. 4. By conducting this optimization for all positions within a plaquette, a map of the optimal impurity placement can be constructed. The results of this are depicted in Fig. 5. See the appendix for the values of δ_{LI} corresponding to these impurity positions.

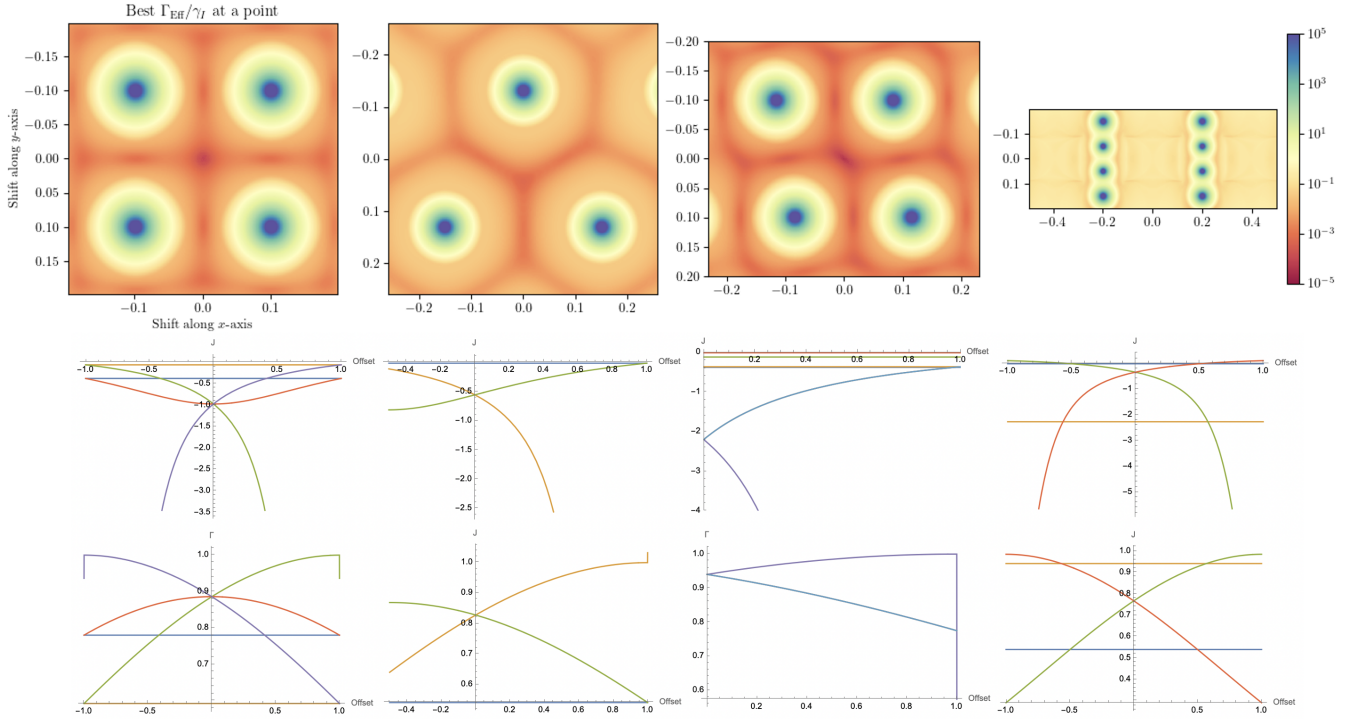


Figure 5. •[To do: 1) Change monoclinic plaquette to something more like theta = 0.4. 2) Change rectangular scaling to something more like 1.5 or 1.3. 4) Update the Mathematica lineplots to match this, because even now, they were made for the wrong theta and scaling. 3) Draw line paths across all the plaquettes, illustrating which paths the plots are graphed over]

In all cases, geometric symmetries determine where the points of minimal Γ_{eff} lie. The paths of minimal Γ_{eff} follow the geometry of a Voronoi diagram constructed around the lattice atoms. The vertices where edges of this Voronoi partition meet are then the points of minimal Γ_{eff} , which are typically the global minima as well. The number of edges that coincide at any one point roughly correlates to how low the effective decay rate will be compared to other such points. For instance, the center of the square plaquette, where four edges coincide, has an optimal Γ_{eff} (7.58×10^{-5} [units]) that is approximately an order of magnitude less than the optimal Γ_{eff} at the center of the triangular plaquette (6.75×10^{-4} [units]), where only three edges coincide. Note that this Voronoi structure does not always result in the center of the plaquette becoming the optimal position for an impurity, as demonstrated by the monoclinic case. The optimal positions are just off of the center, on the line of symmetry along the long axis of the plaquette, at a pair of points where three Voronoi edges meet. As θ approaches $\frac{\pi}{2}$, these two points merge into one, smoothly approaching the minimum found at the center of a square plaquette.

[This suggests that we should try a hexagonal plaquette of the same area, and that we will get an even better result from that! Not a Bravais lattice, but surely still worth a try.]

[Also, it's almost certainly worth mentioning that there is a limit to this Voronoi argument, as shown by the papers on the LHC's of photosynthetic molecules, where the best decay rates are found for polygon plaquettes of nine lattice particles, not "circular polygons" made out of infinite lattice particles for each plaquette.]

The role that symmetry plays in creating these Voronoi geometries is clear once the couplings J_{ij} and Γ_{ij} between pairs of particles are plotted over a path through the plaquette space. At points of geometric symmetry, such as the centers of plaquettes, the values of these couplings coincide. In general, the more that couplings match, the lower the Γ_{eff} for an impurity placed at the point. In this way, lattices with higher degrees of symmetry (i.e. the square and triangular lattices), and with higher numbers of atoms in a single plaquette (i.e. any Bravais lattice other than the triangular lattice) possess impurity positions with the smallest Γ_{eff} . The fact that the square lattice possesses both of these properties helps to explain why it stands out amongst the various Bravais lattices as the optimal choice.

[Look at the "unscaled example.png," and see how it shows that not must the nearest neighbors, but the second-nearest neighbors also matter to ensuring a small Gamma eff

at the center. Then make this point in the paper, that the collective modes are not just governed by nearest neighbors.]

B. Substitutional

Now, considering substituting a lattice atom for an impurity, so that, in effect, the impurity takes up a vacancy in the lattice. In general, the impurity positions available when an impurity is substituted for a lattice atom result in Γ_{eff} that are sub-optimal compared to an interstitial impurity placement (Fig. 6). The best positions for a substitution are also almost always off-center, as an impurity substitution in the exact position of where a lattice atom should be tends to put the Γ_{eff} of the impurity in the region of a local maximum. Offsetting the impurity so that it lies approximately midway between a lattice atom and the vacancy left by the lattice atom that is replaced returns it to a local maximum.

[Can this argument be made more clear if we add high-contrast version of the hexagonal and rectangular plots?]

The symmetry of the lattice is already broken by substituting an offset impurity for a lattice atom, and so symmetry does not play as great a role in determining the optimal impurity position compared to the interstitial case. If there is any role for symmetry, it is between the lattice atoms and the vacancy made by the substitution, so that the impurity receives the best Γ_{eff} when it sits between these points.

[There is surely more to say. For instance, why is the hexagonal case so much worse than the monoclinic case?]

For all Bravais lattices, across all monoclinic angles and rectangular scalings, the optimal Γ_{eff} for a substitutional impurity placement is always greater than the optimal Γ_{eff} for an interstitial impurity. As a result, to optimize for the longest lifetime of the impurity's excited state, an interstitial placement is best for any Bravais lattice.

[Demonstrate this with a figure that shows the optimal Γ_{eff} for all theta and scalings. My current plot is inadequate for this, especially, since it keeps the impurity in the center of the plaquette when the best position for a monoclinic lattice is off-center.]

C. Varying scaling factors

By keeping the impurity at a vertex of the Voronoi partition for all θ within a monoclinic plaquette, a plot of Γ_{eff} over θ and δ can be constructed. As shown in Fig. 10, the optimal δ_{LI} oscillates over θ . In particular, the peaks of this oscillation correlate to the geometries where the impurity is closest to its nearest neighbor amongst the lattice atoms. [comment on lineplots that are yet to be added to this plot, and

how the horizontal-wise minima do or do not reflect the Voronoi conjecture, perhaps].

Regardless of the detailed structure of the local minima over the available range of θ , the global minimum remains at $\theta = \pi/2$, where the monoclinic plaquette is equivalent to the square plaquette, in agreement with the results from our numerical analysis of the plaquette space.

[And just check that all this remains the case when you keep the impurity off-center at its Voronoi maxima]

Likewise, for the rectangular plot, the detrimental effect of varying the scale factor from a value equivalent to the square case at $\mu = 1$ is clear after calculating Γ_{eff} over μ and δ_{LI} . In this case, Γ_{eff} increases rapidly as it approaches the band edge, rectangular scaling changes the minimum of Γ_{eff} by a more direct and destructive mechanism than the monoclinic case. This makes sense geometrically, as varying θ for an infinite lattice merely cycles the lattice through a closed loop of available geometries, while varying μ for an infinite lattice involves no recurrence of any previous geometries for any value of μ . Instead, such a rectangular lattice merely approaches a chain of infinite length, which is, in the end, equivalent to empty space.

In this way, rectangular scaling breaks the ideal square plaquette geometry more rapidly than for the monoclinic case, and again demonstrates that square plaquettes should be favored over rectangular Bravais lattices.

IV. TWO IMPURITY CASE

[Q-factor, analyze different lattices -> discuss the most important figures, constant distance]

Γ_{eff} for a lattice with two impurities is calculated in a manner analogous to the single-impurity case, starting with the Schrödinger equation for the two-impurity Hamiltonian, for which

$$i\hbar \begin{pmatrix} 0 \\ \vdots \\ 0 \\ \dot{c} \\ \dot{d} \end{pmatrix} = \begin{pmatrix} & C_{L1} & C_{L2} \\ H_L & \vdots & \vdots \\ & C_{L1} & C_{L2} \\ C_{1L} & \cdots & C_{1L} & H_1 & C_{12} \\ C_{2L} & \cdots & C_{2L} & C_{21} & H_2 \end{pmatrix} \begin{pmatrix} b_1 \\ \vdots \\ b_N \\ c \\ d \end{pmatrix} \quad (11)$$

In this way,

$$b = -(H_L)^{-1}(C_{L1}c + C_{L2}d) \quad (12)$$

Putting this result back into the Schrödinger equation gives

$$\begin{aligned} \dot{c} &= -i [H_1 - C_{1L}^T(H_L)^{-1}C_{L1}] c \\ &\quad - i [C_{12} - C_{1L}^T(H_L)^{-1}C_{L2}] d \end{aligned} \quad (13a)$$

$$\begin{aligned} \dot{d} &= -i [C_{21} - C_{2L}^T(H_L)^{-1}C_{L1}] c \\ &\quad - i [H_2 - C_{2L}^T(H_L)^{-1}C_{L2}] d \end{aligned} \quad (13b)$$

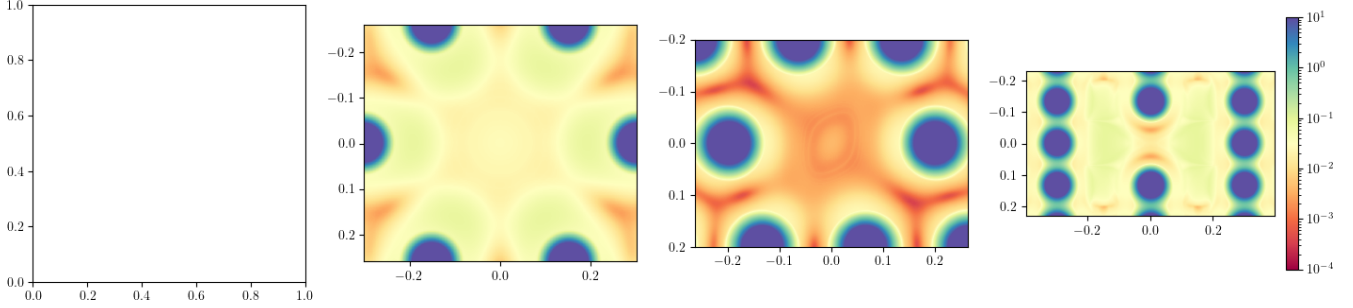


Figure 6. •

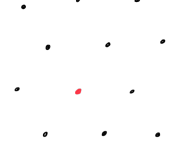


Figure 7. [Merge this with Figure 3? If not, then at least put this earlier.]

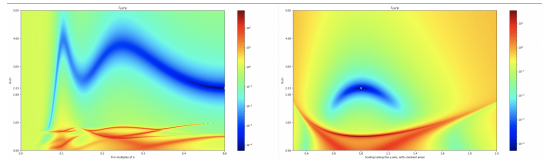


Figure 8. • [Reproduce this plot with the impurity kept at the Voronoi vertices and not at the center. Use the analytical definition of the Voronoi vertices, so that you don't have to optimize for every theta] [ALSO, perhaps put a couple of lineplots just below these plots, that trace along the blue lines, showing where the minima along this line minimum Gamma lie?]

Let $\dot{c} = -i[\Sigma_1 - \frac{i\gamma_1}{2}]c - i\kappa_1 d$ and $\dot{d} = -i[\Sigma_2 - \frac{i\gamma_2}{2}]d - i\kappa_2 c$, where κ_1 and κ_2 are “effective couplings.” Solving for

Figure 9. • [Make a bar plot of the minimal Gamma eff for all eight of the cases considered in this section. Use this to prove that the interstitial case is always better than the substitutional. Also, on the plaquette plot figures, mark where these minima are with an arrow.]

Figure 10. • [placeholder for the figure]

these and the self-energies results in

$$\Sigma_1 = H_1 - C_{1L}^T (H_L)^{-1} C_{L1} + \frac{i\gamma_1}{2} \quad (14a)$$

$$\Sigma_2 = H_2 - C_{2L}^T (H_L)^{-1} C_{L2} + \frac{i\gamma_2}{2} \quad (14b)$$

$$\kappa_1 = C_{12} - C_{1L}^T (H_L)^{-1} C_{L2} \quad (14c)$$

$$\kappa_2 = C_{21} - C_{2L}^T (H_L)^{-1} C_{L1} \quad (14d)$$

The impurities’ effective decay rates are determined by $\Gamma_{\text{eff},i} = \gamma_i - 2 \text{Im}[\Sigma_i]$, where i stands for either the first or second impurity. Likewise, we define the Q-factor as a function of the effective decay rate and the effective coupling, so that $Q_i = \frac{\text{Re}[\kappa_i]}{\Gamma_{\text{eff},i}}$ for each of the two impurities. Because the first and second impurities occupy symmetric positions in the lattice, we find that $\Gamma_{\text{eff},1} = \Gamma_{\text{eff},2}$ and $Q_1 = Q_2$. We thus consolidate these variables, so that we may speak of the impurities’ effective decay rate Γ_{eff} and overall quality factor Q .

As evidenced by the single impurity case, the square plaquette may be taken as a base case, with optimal Γ_{eff} over any other type of Bravais lattice. Because of this, we consider just the square plaquette and the Bravais geometries that smoothly deviate from it, namely the monoclinic and rectangular cases.

[Is it worth ever speaking about the square plaquette two-impurity case on its own? The trouble is, there is precious little to say about it other than how it stands in comparison to the monoclinic and rectangular cases.]

[Also, this last paragraph is a pretty thin argument for why this is missing a section on the triangular case for two impurities. Is it just worth including that case too?]

A. Monoclinic lattice

As θ is varied, the quality factor invariably becomes greater for any deviation from the square lattice at $\theta = \pi/2$. This aligns with the behavior of Γ_{eff} in the single impurity case. That being said, there is also a simple geometric argument that contributes: as θ changes away from $\pi/2$, the distance between the two impurities grows larger. As such, the strength of the interaction between the two impurities decreases, and we are left to conclude, when two impurities are introduced, the square plaquette still performs better than a monoclinic lattice.

B. Rectangular lattice

A rectangular lattice with two impurities has a non-trivial dependence on the scaling factor. While the Γ_{eff} for the two impurities follows the pattern seen in the single impurity case where any deviation from a square plaquette increases the effective decay rate, the quality factor does not adhere to this. Instead, scaling along the axis perpendicular to the axis along which the two impurities lie improves the Q factor from [(quantity)] to [(quantity)]. This behavior does move the two impurities closer to each other, thus enhancing the interaction

between them, and the resultant Q -factor. The behavior can also be heuristically understood by considering the two lines of lattice atoms on either side of the axis of the impurity atoms as two chains that are reshaped by the rectangular scaling. There is then a gain in quality factor due to the increased density of these chains, up to the point of a global minimum found at $\mu = [\text{quantity}]$. As a result, unlike the monoclinic, the rectangular lattice has a global optimum distinct from the square plaquette.

This case demonstrates that the behavior of the quality factor does not always follow naturally from the behavior of Γ_{eff} , and hence that they must both be analyzed separately when analyzing any optical lattice with more than one impurity.

V. CONCLUSIONS AND OUTLOOK

These are the Conclusions.

Acknowledgments. We would like to thank [add people]. This work was supported by [add funding sources]

The numerical simulations were performed with the open-source framework `QuantumOptics.jl` [1].

[1] S. Krämer, D. Plankensteiner, L. Ostermann, and H. Ritsch, `QuantumOptics.jl`: A Julia framework for sim-

ulating open quantum systems, *Computer Physics Communications* **227**, 109 (2018).